Carbon balance and emissions of methane and nitrous oxide during four years of moderate rewetting of a cultivated peat soil site

Kristiina Lång*, Henri Honkanen, Jaakko Heikkinen, Sanna Saarnio, Tuula Larmola, Hanna Kekkonen

5   Natural Resources Institute Finland, Latokartanonkaari 9, FI-00790 Helsinki, Finland

Correspondence to: Kristiina Lång (kristiina.lang@luke.fi)

Abstract. We experimented a gradual water table rise at a highly degraded agricultural peat soil site with plots of willow, forage and mixed vegetation (set-aside) in southern Finland. We measured the emissions of carbon dioxide (CO_2), methane

10   (CH_4) and nitrous oxide (N_2O) for four years. The mean annual ground water table depth was about 80, 40, 40 and 30 cm in 2019-2022, respectively. The results indicated that a 10 cm raise in the water table depth was able to slow down annual CO_2 emissions from soil respiration by 0.87 Mg CO_2-C ha^{-1}. CH_4 fluxes changed from uptake to emissions with a raise in the water table depth, and the maximum mean annual emission rate was 11 kg CH_4-C. Nitrous oxide emissions ranged from 2 to 33 kg N_2O-N ha^{-1} year; they were high from bare soil in the beginning of the experiment but decreased towards the end of the

15   experiment. Short rotation cropping of willow reached net sequestration of carbon before harvest, but all treatments and years showed net loss of carbon based on the net ecosystem carbon balance. Overall, the short rotation coppice of willow had the most favourable carbon and greenhouse gas balance over the years (10 Mg CO_2 eq. on the average over four years). The total greenhouse gas balance of the forage and set-aside treatments did not go under 27 Mg CO_2 eq. ha^{-1} year^{-1} highlighting the challenge in curbing peat decomposition in highly degraded cultivated peatlands.

20

Keywords: peatland, greenhouse gas, ground water table, paludiculture, land use

Graphical abstract
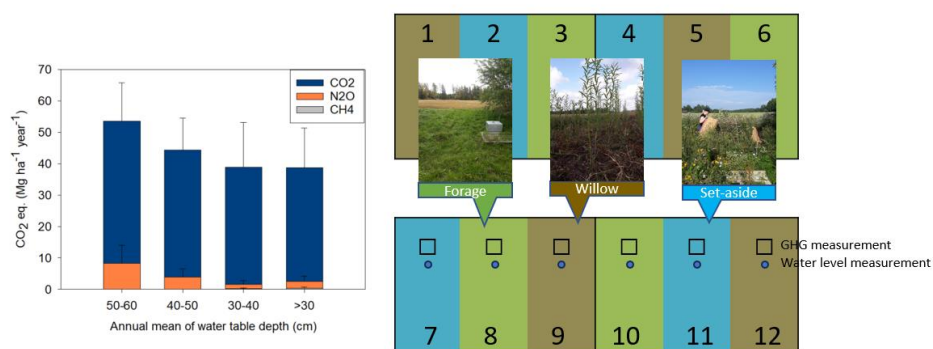
Photos: Jaana Nissi

25

1. Introduction

30   Cultivated peatlands are a major source of greenhouse gas (GHG) emissions globally (Strack et al., 2022). Conventional cultivation requires lowering the water table depth (WTD) which makes all peat above the drainage depth prone to microbial decomposition. Intensive management together with the high carbon and nitrogen content of peat makes agricultural peat soils the highest CO_2 and N_2O emitters per unit area compared to any other land use types on peat soils (Maljanen et al., 2010). Their GHG emissions currently diminish the net carbon sink of peat-rich countries significantly which can also be turned to

35   an advance: the climate change mitigation potential of drained peatlands is high (Humpenöder et al., 2020; Leifeld and Menichetti, 2018) and cost per mitigated unit of CO_2 equivalent low (Lehtonen et al., 2022).

WTD is the major controller of GHG fluxes from peat soils (Evans et al., 2021; Wilson et al., 2016). A global meta-analysis on water table manipulation studies showed that WTD explained most of the variation in GHG emissions but e.g. climate zone had some influence as well (Huang et al., 2021). Rewetting has been found to diminish the release of CO_2 and N_2O from

40   decomposition but the switch from aerobic to anaerobic decomposition may change the ecosystem from a sink to source of CH_4. However, the average increase in CH_4 emissions does not compromise the net GHG mitigation potential (Bianchi et al., 2021; Guenther et al., 2020; Mander et al., 2023).

Paludiculture, crop production in wet conditions, is a GHG mitigation method that allows for slowing down peat decomposition while still maintaining agricultural income from peatlands for the landowner (Tanneberger et al., 2022). It is an opportunity

45   for the agribusiness to improve the overall sustainability (Freeman et al., 2022; Liu et al., 2023) and it produces clearly more societal benefits in the form of ecosystem services than conventional management (Liu et al., 2023). As regards GHG mitigation, the raise in WTD reduces carbon losses from peat decomposition but export of carbon in the harvest impairs the carbon balance of the system (Beetz et al., 2013). Emissions of N_2O are generally found to be low in paludiculture (Bianchi et al., 2021) but they can remain high if fertilisers are applied (Bockermann et al., 2024). Emissions of CH_4 are affected by the

50   crop type, harvest management and N fertilisation (Boonman et al., 2023) but they can be efficiently reduced by leaving an oxidised layer on the peat surface (Kandel et al., 2020).

We established an experimental site with forage, willow and set-aside treatments in wet management on highly decomposed cultivated peat soil in southern Finland in 2019-2023. As the target WTD of -20 cm below the surface was reached only periodically, we cannot call the site a paludiculture site, but the results can be used to discuss the effects and practical issues

55   during the transition period to paludiculture. Our research questions were 1) What is the carbon and GHG balance of a moderately rewetted drained peatland, 2) How much does harvesting reduce the potential to improve the carbon balance and 3) Do CH_4 emissions compromise the GHG mitigation in wet management?

60   ## 2. Materials and methods

2.1. The site and management

The site was located in southern Finland (60.22 ⁰N, 24.78 ⁰E, 110 m a.s.l.) and it has been in cultivation at least since the 19th century. The field has been in a crop rotation with cereals and grass during the latest decades. The climate is boreal humid with long term (1991–2021) annual mean temperature of 5.2 ˚C and precipitation of 621 mm (Jokinen et al. 2021). The sum

65   of annual global radiation is 3358 MJ m^{-2} and total sunshine duration 1699 hours. Typically, the soil is frozen and has a snow cover from December to March-April. The field was a highly decomposed fen with peat depth ranging from 0.8 to over 2 m. Organic carbon content was 25% and pH 5.5 in the surface layer (0–20 cm) (Table 1). The original subsurface drainage system with tile drains was replaced by modern plastic pipes surrounded by gravel in the 1960s. The distance between the pipes was

18 m until 1979 when it was changed to 9 m. The drainage depth was 60–80 cm, and prior to the experiment a control well
70   was installed to restrict water outflow and raise the ground water table.

Table 1: Soil properties in the 0-20 cm layer in 2021

Variable	Value ±sd
Decomposition status (von Post)	8 (7-9)
Bulk density (g cm-3)	0.39±0.05
Porosity (%)	0.80±0.02
Ash (%)	42±3.8
pH	5.4±0.09
C (g kg^{-1})	286±24.6
N (g kg^{-1})	15.2±1.24
Tot P (g kg^{-1})	0.97±0.08
Soluble P (g kg^{-1})	0.01±0.001
K (g kg^{-1})	0.17±0.03
Mn (g kg^{-1})	0.15±0.02
S (g kg^{-1})	2.01±0.13
Al (g kg^{-1})	1.41±0.12
Fe (g kg^{-1})	5.92±0.63

Twelve experimental plots (9 × 6 m) were established in 2018. Four replicate plots with either grass mixture for forage (sown
75   with *Poa trivialis* and *Festuca pratensis*, replanted in 2019 and 2021 with *Phleum pratense, Festuca pratensis, Lolium
multiflorum and Poa pratensis*), bog bilberry (*Vaccinium uliginosum*; aka bog blueberry or bog whortleberry) or willow variety
Klara (hybrid of *Salix schwerinii* Amgunskaja x *Salix viminalis* Ivar) were randomly assigned within four blocks (see the
graphical abstract). The grass was seeded and bilberry seedlings and willow saplings planted in June 2018 (Table S1). The
bilberry did not grow roots, and those plots were left to develop to set-aside during the following years, thus we named this
80   treatment as "set-aside". The number of species in the set-aside plots was determined once in the summer 2021.

2.2 Ancillary measurements

Biomass growth of willow was monitored by cutting three willow individuals from each plot for determining the above-ground
biomass each June. The leaves, and stem + branches were separated and weighed to determine the fresh biomass. The woody
85   biomass was cut in 10 cm pieces and dried at 65 °C for two weeks. The root biomass around one of the monitored plants per
plot was determined by taking 50 × 80 × 20 cm peat samples from three layers: 0–20, 20–40 and 40–60 cm once per year.
Visible large (>2 mm) and fine roots were manually separated from the peat, dried and weighed. For determining fine roots,
the peat samples were mixed, and a 1 kg subsample was taken. Annual growth in stem, stool and coarse roots was calculated
by subtracting the value from the previous year. Annual turnover rate of fine roots was assumed to be three times the biomass
90   of fine roots as in Pacaldo et al. (2014). For example, biomass increment in 2019 was calculated with the following equation:

$$Annual\ Growth = F_{19} + (S_{20} - S_{19}) + (St_{20} - St_{19}) + (Cr_{20} - Cr_{19}) + 3 * Fr_{19} \qquad (1)$$

, where F19 is foliage in 2019, S19 and S20 are stems in 2019 and 2020, St19 and St20 are stools in 2019 and 2020, Cr19 and
95   Cr20 are coarse roots in 2019 and 2020 and Fr19 is fine roots in 2019. Subsamples were taken for determining the C content
of the dried biomass in 2019 and 2020, and the mean values were used for the following years. The yield per hectare was
estimated to be the weight of 25,000 individuals, based on 80 cm × 50 cm spacing.
Soil temperature was measured first at the depth of 10 cm (but at the depth of 5 cm from May 2020 on to achieve better
response of CO_2 to air temperature) in each treatment with Elcolog sensors (Elcoplast Oy, Tampere, Finland). The sampling

rate was one hour in summer and 2.5 hours in winter. The air temperature, precipitation and radiation data were taken from the weather station of Finnish Meteorological Institute (FMI, CC BY 4.0) located about 10 km from the site. Continuous photosynthetically active radiation (PAR) data was produced with global radiation data from FMI and corrected using the ratio of 2.04 for global radiation and the PAR (Meek et al., 1984).

WTD was measured from monitoring pipes at the corners of the experimental area at the time of the opaque chamber measurements until 2021 when monitoring pipes were installed also in centre of each plot. During summers 2021 and 2022, there were also HOBO Water Level data loggers (Onset, Bourne, United States) in each plot for continuous water level monitoring with a sampling rate of one hour. In winter when the loggers were not used, WTD was measured manually from monitoring pipes when possible.

Leaf area index (LAI) was measured at the same time with the transparent chamber measurements with a portable LAI meter (SunScan; Delta-T Devices Ltd, Cambridge, United Kingdom). LAI values > 3 were set to 3 as they were assumed to not affect photosynthesis due to saturation of the reflectance (Aparicio et al., 2000). When harvesting the grass plots, the previous measured LAI value was extrapolated to the moment just before harvesting, after which the LAI value was set to 1 as measured. In 2022, we measured green canopy cover instead of LAI, because it responded better to photosynthesis. Green canopy cover was measured with the Canopeo app (Oklahoma State University Department of Plant and Soil Sciences, Stillwater, United States). LAI was indexed by dividing by maximum value 3 and green canopy cover by 100 (values from 0% to 100%) so that the generated vegetation index range was 0–1. The vegetation index was set to 0 from the end of November until mid-April when the snow and frost covered the ground or no green vegetation occurred.

Soil samples for analysing the soil properties were taken first in October 2018 and another sampling was conducted in June 2021 with additional analysis. As there were no significant changes in the soil properties between these samplings, we present only the results of the second soil sampling in Table 1. The samples were taken from the 0-20 cm layer using a soil corer with a diameter of 3 cm. Approx. 20 subsamples were pooled to make composite sample that was air-dried and sieved (2 mm) for the chemical analyses. Soil core samples for dry bulk density and porosity (diameter 5 cm) were taken from the surface layer (0–17.5 cm) of each plot in Oct 2020 using the Kopec corer, and the samples were dried at 37 °C for a week. Soil acidity was determined using the ISO 10390 method. Nutrient content was analysed as described in Vuorinen and Mäkitie (1955). Soil carbon and nitrogen were determined using the dry combustion method (Leco TruMac CN, LECO corporation, MI).

2.3. GHG measurements

The GHG fluxes were measured using four different methods: opaque chambers, transparent chambers, snow gradient method and small soil respiration chambers. Between 3/2019 – 3/2023, opaque chambers were used to measure ecosystem respiration, N_2O and CH_4. In each plot, a 60 cm × 60 cm steel collar was installed at the depth of 10–15 cm. The location of the collars was one metre from the short edge of the plot and three metres from the edges of the adjacent plots. An aluminium chamber (height 40 cm) mounted at the top of the collar was sealed with water in the groove of the upper edge of the collar. In the winter, NaCl was added to the water to avoid ice formation. The clear aluminium surface reflected effectively light and kept the temperature change moderate inside the chamber. The measurements were done during the daytime between 10 am and 2 pm approximately biweekly in summertime, and monthly in the winter. The chambers were closed for 30 minutes, and four 20 ml gas samples were taken with a 60-ml plastic syringe to pre-evacuated vials (Exetainer, Labco Limited, UK) in 10-minute intervals starting immediately after closing. Prior to sampling, the syringe was pumped five times to mix the air in the chamber. The samples were analysed with a gas chromatograph (Agilent 7890 Agilent Technologies, Inc., Wilmington, DE, USA) equipped with flame ionizer and electron capture detectors, and a nickel catalyst for converting CO_2 to CH_4. The gas chromatograph had a 2 ml sample loop and a backflush system for separating water from the sample and flushing the precolumn between the runs. The precolumn and analytical columns consisted of 1.8 and 3 m long steel columns, respectively, and were

packed with 80/100 mesh Hayesep Q (Supelco Inc., Bellefonte, PA, USA). Nitrogen was used as the carrier gas and a standard gas mixture of known concentration of CO_2, N_2O and CH_4 was used for a calibration curve with seven concentration points. An autosampler (222 XL Liquid handler, Gilson Medical Electronics, France) fed the samples to the loop of the gas

145 chromatograph.

A transparent chamber ($60 \times 60 \times 60$ cm) made of polycarbonate plexiglass (1 mm, light transmission 95%) was used to measure net ecosystem exchange (NEE) approximately biweekly during the growing season. The chamber was equipped with a Vaisala GMP-343 probe and a temperature and humidity sensor (Vaisala Oy, Vantaa, Finland) and two fans for mixing the air during the measurement. PAR was measured with LI-190 quantum PAR sensor (LI-COR, Lincoln, Nebraska, USA) inside

150 the chamber. One or two layers of a white fabric shroud and one blackout curtain were used to control the amount of light entering the chamber (approximately 100%, 50%, 25%, 0% of ambient radiation). The measurements were done in the same collars as the opaque chamber measurements. Four measurements with different amount of entering light were taken from each subplot in order to cover a large range of light conditions. Each measurement took one minute with a five second sampling rate, or two minutes in early or late growing season when the change in flux was minor. The chamber was flushed after each

155 measurement to reconstitute ambient CO_2 and air humidity contents. After closing the chamber, a lag time of 10 seconds was applied to exclude the time when the flux was not yet stabilised. Clear sky conditions were preferred to avoid problems related to changing cloud cover and to achieve the widest possible range of available light. The temperature change inside the chamber was less than 1.5 degrees which was also used as a criterion for data filtering.

The change of CO_2 concentration during the chamber enclosure was assumed to be linear. The measurement results of CO_2 as

160 parts per million (ppm) unit were converted to g m^{-2} h^{-1} by the ideal gas law using measured temperature inside the chamber. If the flux was not yet stabilized at the beginning (first 4 datapoints) of the measurement, outliers were defined with Matlab isoutlier command resulting removal of 210 of total 23066 datapoints in 1564 flux measurements.

If the snow cover was thicker than 20 cm, a concentration snow gradient method as in Maljanen et al. (2003) was used to determine the GHG fluxes. A probe made of a steel pipe (Ø 3 mm), with a three-way valve and a plastic syringe, was used to

165 sample 15 ml of air just above the snow cover, in the bottom of the snow cover and at every 10 cm in between in three replicate locations per plot. The gas was stored in the pre-evacuated vials and the concentrations were determined gas chromatographically.

Measurements for bare soil respiration were made in 7/2019–12/2022. We installed one sheet metal air ventilation pipe 27 cm in diameter and 30 cm in length to the depth of 5–10 cm in the 8 subplots of grass and set-aside plots next to the opaque

170 chamber collars. All green vegetation within the chamber area was removed and root growth was limited by cutting around the chamber occasionally with a knife. For the measurements, the cylinders were closed with a cover equipped with a CO_2 sensor (GMP-343; Vaisala Oyj, Vantaa, Finland) and a small fan. One measurement lasted for one minute with a five second sampling rate. Measurements were taken about once in a week or two, more frequently in summer than in winter. In winters 2021 – 2022 and 2022 – 2023 this method was not used due to too high snow depth but measurements with the snow gradient

175 method were utilized (Maljanen et al., 2003).

2.4. Flux modelling

NEE is the difference in the gross fluxes gross photosynthesis (GP) and ecosystem respiration (ER). Instantaneous GP was estimated for each NEE measurement by (equation 2),

180

$$GP = NEE - ER \qquad (2)$$

, where the full darkened transparent chamber measurement result (ER) is subtracted from the light-dependent flux (NEE) measured during the same day. Thus, we follow the sign convention with positive ER and negative GP values.

185 Annual ER and GP (April to March) were modelled using nonlinear regression (fitnlm function in MATLAB 2019b) for all 8 plots in forage and set-aside treatments. Empirical models were used for ER as in Lohila et al. (2003) and for GP as in Kandel et al. (2013). Instead of the phytomass indices used in the above publications, we used vegetation index (index from 0 to 1) to describe the stage of the crop growth. Air temperature and PAR were assumed to be the same for all plots, whereas we used plot specific vegetation index and the soil temperature from the certain treatment.

190 We used the following equation defined by Long and Hällgren (1993) for GP to estimate empirical coefficients (A_{max} and k):

$$GP = \frac{A_{Max}*PAR}{k+PAR} * VI * T_{Scale} \qquad (3)$$

, where PAR is the measured photosynthetically active radiation, VI is the vegetation index, A_{max} is the asymptotic maximum,

195 and k is a half-saturation value. T_{Scale} represents the temperature sensitivity of photosynthesis and follows the equation presented by Raich et al. (1991):

$$T_{Scale} = \frac{(T-T_{min})(T-T_{max})}{(T-T_{min})(T-T_{max})-(T-T_{opt})^2} \qquad (4)$$

200 , where T is the measured temperature, photosynthetically active minimum temperature T_{min} is -2 ˚C, maximum T_{max} is 40 ˚C and the optimum is 20 ˚C as in Kandel et al. (2013).

ER consists of autotrophic (R_{auto}), i.e., plant respiration and heterotrophic (R_{hetero}), i.e., soil respiration (Lloyd and Taylor, 1994) with extension of WTD as in Karki et al. (2014):

205 $$ER = R_{hetero} + R_{auto} \qquad (5)$$

$$R_{hetero} = R0_s * \exp\left(E0_s \left(\frac{1}{56.02} - \frac{1}{T_{soil}+46.02}\right)\right) + b * WTD \qquad (6)$$

$$R_{auto} = VI * R0_p * \exp\left(b_d\left(\frac{1}{10+273} - \frac{1}{T_{air}+273}\right)\right) \qquad (7)$$

, where T_{soil} is the measured soil temperature, VI is the vegetation index, T_{air} is the measured air temperature, $R0_s$ is soil

210 respiration at the reference temperature 10 ˚C, $R0_p$ is plant respiration at the reference temperature at 10 ˚C, b is the effect of WTD, $E0_s$ is ecosystem sensitivity and b_d was the temperature dependence of dark respiration set to 5000 as in Lohila et al. (2003).

ER was estimated using data from opaque and fully darkened transparent chambers. The empirical coefficients ($R0_s$, $R0_p$, $E0_s$ and b_d) were estimated with a nonlinear regression model similarly as in the case of GP. Hourly timeseries of GP and ER were

215 predicted with the above equations using the modelled parameters and hourly timeseries of the field measurements. Hourly time points for vegetation index, WTD and soil temperature and were acquired from the measured values by linear interpolation. Gaps in soil temperature were filled with the modified soil temperature model (Zheng et al., 1993) using the air temperature. Annual fluxes were computed as integral of the hourly fluxes with a trapezoidal method (trapz function in Matlab).

220

2.5. Data processing and analysis

For the transparent chamber measurements, the criteria $R^2 > 0.9$ for the fitted linear assumption of flux measurements would exclude a large amount of data, especially with a small change in CO_2, leading to a biased dataset. Therefore, we decided to add the criterion $S_{xy} < 2.3$ g CO_2 m^{-2} h^{-1} for dataset as in Kutzbach et al. (2007) (S_{xy} is the standard deviation of the residuals and 2.3 g m^{-2} h^{-1} is the 95% percentile of measurements). This procedure resulted in the removal of 59 values out of total 1467 measurements. In the modelling phase, fitted values were examined, and outliers were removed to avoid distortion. Outliers were defined as observations with an absolute value of standardised residuals greater than three. In 2019, 3 out of 260 GP values and 3 of 243 ER values were removed. In 2020, none of 200 GP values and 2 of 230 ER values were removed. 2 out of 365 GP values and 4 of 247 ER values were removed in 2021 and 12 out of 583 GP values and 2 of 323 ER values were removed in 2022. The model's estimated parameters A_{max}, k of GP, $R0_s$ and $R0_p$ of ER and model correlations are shown in Table S2. The measured versus model predicted values of GP and ER are shown by treatments and years in Fig. 2.

For bare soil respiration measurements in set-aside and forage, the same criteria was used as for transparent chamber ($R^2 > 0.9$ and $S_{xy} < 95\%$) leading a removal of 12 values of total 601. In bare soil measurements in midsummer 2022, there occurred 24 flux measurements (9 values in one plot, 0-5 in others) of total 147 values which were unexplained high ($3 – 18$ g CO_2 m^{-2} h^{-1}). Values were of the same magnitude as values measured immediately after ploughing in Honkanen et al. (2023). We decided to remove these values as outliers to avoid model distortion. Soil respiration of willow was defined with opaque chamber method and such outliers did not occur in these measurements. In modelling phase, outliers defined as observations with an absolute value of standardised residuals greater than three, were removed resulting removal of 13 measurements of total 984 measurements (including all plots).

A linear regression model was fitted to calculate gas concentrations and the ideal gas law was used to solve the flux rate for every enclosure of the opaque chambers. Nonlinear responses of CO_2 indicated a leaking chamber or other problem in the measurement and thus, if the R^2 of CO_2 was less than 0.9, also the results of CH_4 and N_2O were discarded. In addition, sudden variations in CH_4 fluxes due to ebullition were filtered by selecting only flux rates with the intercept between 1.5 and 2.4 ppm. These criteria resulted to 176, 117 and 118 discarded values out of 1044 in the case of CH_4, CO_2 and N_2O, respectively. The cumulative annual fluxes for each management practice were calculated by interpolating the emissions between consecutive sampling days. Global warming potentials 27 and 273 were used for CH_4 and N_2O, respectively, to convert the results to CO_2 equivalents (Forster et al. 2021).

2.6. Statistical analyses

Linear mixed models were used to find variables explaining variation in the gas fluxes. Crop, year, WTD and all their interactions were denoted as fixed effects. Block and block × year were assumed to be independent and normally distributed random effects. The most suitable covariance structure was chosen using Akaike's Information Criterion (AIC). The models were fitted using the residual maximum likelihood (REML) method and degrees of freedom were estimated using the Kenward-Roger method. The residuals were plotted against the fitted values and the normality of the residuals were checked using boxplots. The differences between treatments were also tested using the ANOVA procedure for each year separately. The data was log- or ln-transformed when needed to normalise the distributions. The method of Tukey-Kramer was used for all pairwise comparisons of means with a significance level of 0.05. All statistical analyses were performed using the SAS Enterprise Guide v7.1 (SAS Institute Inc., Cary, NC, USA).

3. Results

3.1 Climate and site variables

Annual mean temperature was 6.9, 6.0, 5.8 and 5.8 °C and annual precipitation 750, 600, 660, and 546 mm in 2019 – 2022, respectively. Number of days with a snow-cover on the soil was 13, 81, 108 and 118, respectively. The annual mean temperature during the study years was higher than the long-term average of 5.2°C in 1991–2020 (Jokinen et al., 2021). Two study years exhibited lower and two higher annual precipitation as compared to the long-term mean of 621 mm. The WTD showed an increasing trend in time and high within-year variation (Fig. 1). The average WTD was -54, -41, -39 and -27 cm in 2019–2022, respectively. WTD varied from -89 to -4, -77 to 2, -120 to 1.4 and -100 to 1.8 cm in 2019 – 2022, respectively. The forage yields were 6.3±0.9, 8.9±0.7, 11±0.8 and 9.4±0.9 Mg DM ha^{-1} in 2019-2022, respectively. There were two harvests in 2020 and three in the other years. The plots were dominated by *Phleum pratense* and *Festuca pratensis* in 2021. The dry mass yields of willow were 30±14 and 73±28 Mg DM ha^{-1} in the harvests of February 2021 and 2023. Most of the C accumulation occurred in the stem (59%), followed by stool (25%) and roots (9%) and foliage (7%) (Table 2). There were 18 different plant species in the set-aside plots in 2022. Vegetation of the set-aside plots in 2021 was dominated by wild plants belonging to Families *Asteraceae*, *Cichoriaceae* and *Caryophyllaceae*. Bog bilberry covered one percentage or less on each of the four replicate plots. The set-aside vegetation had the highest species diversity, 19 vascular plants compared to 12 at willow plots and 9 at forage plots, the two latter including crop plants.

Table 2: Four-year cumulative carbon balance of willow. Negative sign indicates sequestered carbon and positive sign released carbon to the atmosphere.

Component	Mg C ha^{-1} 4 yrs^{-1}	STD	% of total
Stem (harvested)	-50.7	14.3	59
Foliage	-6.2	0.8	7
Aboveground stool	-12.6	3.2	15
Underground stool	-8.5	3.8	10
Coarse roots	-3.9	1.5	4
Fine roots	-4.6	0.6	5
Total sequestered carbon	-86.5	19.5	
Soil respiration	43.5	2.7	
Net ecosystem exchange	-43.1	21.1	
Net ecosystem carbon balance	7.6	7.7	

285
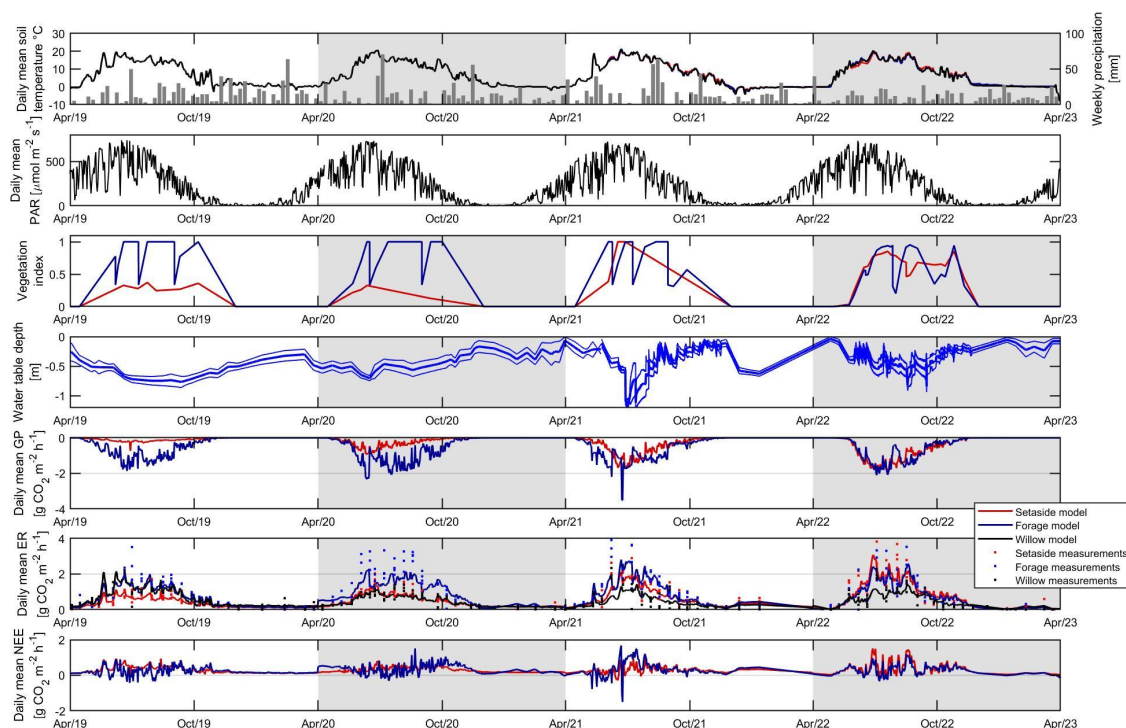
Figure 1: Daily mean of soil temperature and precipitation (a), photosynthetically active radiation (PAR) (b), vegetation index (c), water table depth (site mean±std) (d), measured and model predicted ecosystem respiration (soil respiration for willow) (e), gross photosynthesis (f) and net ecosystem exchange (g). Annual modelling periods (Apr - Apr) are marked with light grey or white background.

3.2. Carbon balance

Model predicted maximum hourly GP was 0.7, 3.2, 4.3 and 4.8 g CO_2 m^{-2} h^{-1} in the set-aside in 2019 – 2020, and 3.9, 5.9, 4.3 and 4.8 g CO_2 m^{-2} h^{-1} in the forage plots in 2019–2022, respectively (Fig. S1). Maximum measured GP value was 1.1, 2.4, 3.4 and 4.5 g CO_2 m^{-2} h^{-1} for set-aside and 3.4, 6.2, 4.8 and 4.2 g CO_2 m^{-2} h^{-1} for forage in 2019–2020, respectively. Annual values of GP varied from 9.3 to 12 Mg CO_2-C ha^{-1} yr^{-1} in the forage and from 1.5 to 10 Mg CO_2-C ha^{-1} yr^{-1} in the set-aside treatment (Table 3). WTD explained variation in GP (p=0.011), but forage and set-aside treatments did not differ significantly. However, there was an interaction between the treatment and WTD indicating that WTD affected GP of the set-aside treatment more than that of the forage (p=0.008).

Table 3: The estimated annual sums (±standard deviation) of gross photosynthesis (GP), ecosystem respiration (ER), net ecosystem exchange (NEE), carbon exported in the harvested yield, net ecosystem carbon balance (NECB), N_2O and CH_4 effluxes and the total emissions (global warming potential of one hundred years; GWP-100) with either NEE or NECB representing CO_2 emissions in the forage and set-aside plots, and selected data for willow. Significant differences (p<0.05) between treatments within a year are denoted with different letters (n=4).

Year	Variable and unit	Forage	Set-aside	Willow
2019	GP Mg CO_2-C ha^{-1}	-9.31±0.75a	-1.48±0.32b	
	ER Mg CO_2-C ha^{-1}	14.4±2.17a	8.25±2.40b	
	NEE Mg CO_2-C ha^{-1}	5.08±1.80	6.77±2.41	
	C in yield Mg C ha^{-1}	3.17±0.49	0	
	NECB Mg C ha^{-1}	8.25±2.13	6.77±2.41	
	Soil respiration Mg CO_2-C ha^{-1}	12.8±4.99	11.4±1.82	14.8±0.76
	N_2O-N kg ha^{-1}	11.9±7.60a	32.6±12.1b	17.4±10.3
	CH_4-C kg ha^{-1}	-0.28±0.75	-1.00±0.73	-1.64±0.26
	GWP$_{100}$ Mg CO_2eq ha^{-1} (NEE)[a]	23.7±5.67	38.8±19.8	
	GWP$_{100}$ Mg CO_2eq ha^{-1} (NECB)[b]	35.3±6.86	38.8±19.8	
2020	GP Mg CO_2-C ha^{-1}	-11.7±1.17a	-3.57±0.46b	
	ER Mg CO_2-C ha^{-1}	19.3±1.85a	10.6±1.49b	
	NEE Mg CO_2-C ha^{-1}	7.64±1.75	7.05±1.12	
	C in yield Mg C ha^{-1}	3.35±1.28	0	
	NECB Mg C ha^{-1}	11.0±2.02	7.05±1.12	
	Soil respiration Mg CO_2-C ha^{-1}	9.09±4.86	10.6±0.97	10.0±0.79
	N_2O-N kg ha^{-1}	6.26±3.39	6.59±2.97	4.61±2.99
	CH_4-C kg ha^{-1}	-0.36±0.40	-1.01±0.56	-1.13±0.33
	GWP$_{100}$ Mg CO_2eq ha^{-1} (NEE)	30.4±7.64	28.7±3.73	
	GWP$_{100}$ Mg CO_2eq ha^{-1} (NEBC)	42.6±8.69	28.7±3.73	
2021	GP Mg CO_2-C ha^{-1}	-9.46±1.20a	-6.34±0.68b	
	ER Mg CO_2-C ha^{-1}	17.4±1.40a	13.5±1.82b	
	NEE Mg CO_2-C ha^{-1}	7.95±2.16	7.12±2.16	
	C in yield Mg C ha^{-1}	5.54±0.46	0	
	NECB Mg C ha^{-1}	13.5±1.88a	7.12±2.16b	
	Soil respiration Mg CO_2-C ha^{-1}	7.82±2.30	11.5±2.44	8.99±2.70
	N_2O-N kg ha^{-1}	6.49±3.88a	2.18±0.24b	5.75±6.25
	CH_4-C kg ha^{-1}	7.92±12.7	0.58±1.87	3.89±6.12
	GWP$_{100}$ Mg CO_2eq ha^{-1} (NEE)	32.2±8.16	27.1±8.03	
	GWP$_{100}$ Mg CO_2eq ha^{-1} (NEBC)	52.2±6.93	27.1±8.03	
2022	GP Mg CO_2-C ha^{-1}	-9.34±2.13	-9.65±2.08	
	ER Mg CO_2-C ha^{-1}	14.4±3.29	16.5±3.21	
	NEE Mg CO_2-C ha^{-1}	5.10±1.15	6.82±1.15	
	C in yield Mg C ha^{-1}	4.72±0.50	0	
	NECB Mg C ha^{-1}	5.46±6.37	6.82±1.15	
	Soil respiration Mg CO_2-C ha^{-1}	8.40±1.48	15.0±5.32	9.70±2.3
	N_2O-N kg ha^{-1}	9.54±4.49a	3.07±0.86b	1.69±1.10b
	CH_4-C kg ha^{-1}	7.74±0.59	11.3±7.72	10.9±12.9
	GWP$_{100}$ Mg CO_2eq ha^{-1} (NEE)	22.9±3.34	26.6±4.61	
	GWP$_{100}$ Mg CO_2eq ha^{-1} (NEBC)	43.3±3.18	26.6±4.61	

[a]With NEE representing CO_2, [b]With NEBC representing CO_2

310   Modelled maximum hourly ER was 2.4, 2.3, 3.0 and 4.7 g CO_2 m^{-2} h^{-1} in the set-aside and 3.5, 3.4, 4.8 and 4.5 g CO_2-C m^{-2} h^{-1} in the forage plots (Fig. S1). Measured maximum ER with the opaque chamber method was 1.7, 2.0, 2.9 and 4.6 g CO_2-C m^{-2} h^{-1} for the set-aside and 3.5, 4.2, 4.0 and 4.8 g CO_2-C m^{-2} h^{-1} for forage. Annual ER varied from 14 to 19 Mg CO_2-C ha^{-1} yr^{-1} in the forage and from 8 to 17 Mg CO_2-C ha^{-1} yr^{-1} in set-aside treatment (Table 3). WTD did not well explain the variation in the annual ER estimate (p=0.062), and the forage and set-aside treatments did not differ significantly. However, there was an

315   interaction between the treatment and WTD indicating that WTD affected ER of the set-aside treatment more than that of the forage (p=0.032).

Hourly model-predicted NEE varied from -2.9 to 3.7 g CO_2 m^{-2} h^{-1} in the set-aside and from -4.6 to 3.7 g CO_2 m^{-2} h^{-1} in the forage treatment (results not shown). There were 29, 28, 16 and 47 days annually with negative daily NEE in the forage plots during the study years, respectively, and fewer such days (1, 0, 9 and 6) in the set-aside plots in 2019–2022 (Fig. 1). The

320   cumulative annual balance ranged from 5.1 to 8.0 Mg CO_2-C ha^{-1} yr^{-1} in the forage and from 6.8 to 7.1 Mg CO_2-C ha^{-1} yr^{-1} in the set-aside treatment (Table 3) and the treatments did not differ statistically. The net ecosystem carbon balance (NECB) that accounts the amount of carbon exported in the harvested yield varied from 5.5 to 13.5 Mg CO_2-C ha^{-1} yr^{-1} in the forage treatment and were equal to NEE in the set-aside treatment (Table 3). The NECB values differed statistically between the forage and set-aside treatments across all years (p>0.001).

325   Annual sum of respiration varied from 8 to 15 Mg CO_2-C ha^{-1} yr^{-1} in the different treatments and years (Table 3). The proportion of soil respiration of the total ecosystem respiration varied from 45 to 90% in the forage plots and from 85 to100% in the set-aside plots in 2019–2022. In the set-aside plots, estimated annual bare soil respiration exceeded the estimated ER in all plots in 2019, two plots in 2020 and one plots in 2021 and 2022 and those values were not used in the above calculation, and thus it is assumed that total respiration constituted only of soil respiration in 2019. Annual cumulative soil respiration was explained

330   by the WTD (Fig. 2; p=0.053) and crop type (p=0.033) so that forage and set-aside treatments were significantly different in the whole dataset. Plots of the bare soil respiration in relation to WTD and temperature show that there is a clear trend of decreasing respiration with raising WTD (Fig. S2). Three individual curves indicate a contrasting trend, but these three estimations are based on a small number of measurement results. Based on all annual estimates of soil respiration, a 0.1 m raise in WTD reduces respiration by 0.87 Mg CO_2-C ha^{-1} yr^{-1}.

335   The cumulative total amount of C in the above and below ground willow biomass was 86.5 Mg C ha^{-1} during the four study years (Table 2). About 40% of the carbon in the biomass was left at the site after harvest, and soil respiration amounted to 43.5 Mg ha^{-1}, leading to a strongly negative cumulative NEE of -43 Mg ha^{-1}. Carbon export in the harvest changed the net balance to net loss of 7.6 Mg, corresponding to an average annual CO_2 rate of 7 Mg of CO_2.
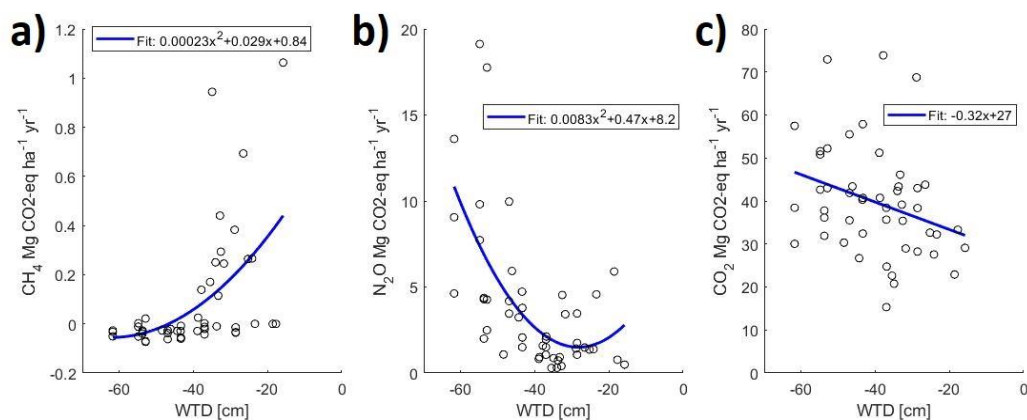
340

Fig. 2. Mean annual fluxes of CH_4 (a), N_2O (b) and soil respiration (c) in CO_2 eq. as related to the mean annual WTD.

3.3. CH₄ fluxes

345 Hourly fluxes of CH_4 varied between -50 and 30 µg CH_4-C m^{-2} h^{-1} during the first half of the experimental period (Fig. 3). In conjunction with the raise in the WTD the values the hourly fluxes increased and varied between -40 and 900 µg m^{-2} h^{-1} during the latter half of the period. The annual flux of CH_4 varied from -1.6 to 11 kg CH_4-C ha^{-1} yr^{-1} with an increasing trend towards the end of the measurement period (Table 3). Variation in the annual cumulative fluxes of each plot was explained by the WTD
350 (p=0.049) but not by crop or year. When the mean annual WTD was below 40 cm the soil was mainly consuming CH_4, but the consumption tended to change to emissions as the WTD raised (Fig. 2).

3.4. N₂O fluxes

Hourly fluxes of N_2O varied between -3 and 2500 µg N_2O-N m^{-2} h^{-1} during the four years with the highest emissions during
355 the first four months (Fig. 3). Annual fluxes of N_2O varied from 1.7 to 33 kg N_2O-N ha^{-1} yr^{-1} (Table 3). The emissions declined in time in the case of set-aside and willow whereas those of forage did not show such a trend. WTD explained variation in N_2O fluxes well (p=0.027) (Fig. 2). Annual N_2O fluxes of the forage and willow treatments differed in the whole timeseries (p=0.011).
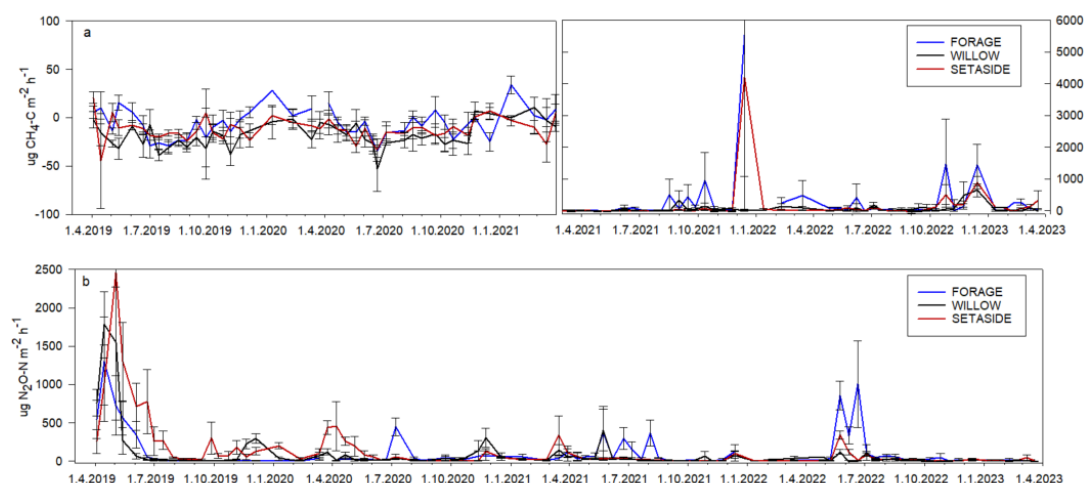
360

Fig. 3. Fluxes of CH$_4$ (a) and N$_2$O (b) in 2019-2023. The error bars denote standard error. Note the different scale in the y-axis of (a) for the latter half of the period.

3.5. Global warming potential

365 The total emissions expressed as CO$_2$ equivalents ranged from 23 to 39 Mg ha^{-1} yr^{-1} with NEE as the CO$_2$ component and from 27 to 52 Mg with the C export in harvest taken into account in the forage and set-aside treatments (Table 3). Based on the four-year estimate, the average annual climate impact of willow cultivation, taking into account the NECB together with average N$_2$O and CH$_4$ fluxes was 10.2 Mg ha^{-1} yr^{-1} (results not shown).

370

2. Discussion

3.1 Forage

NEE values of 5–8 Mg C ha^{-1} per year in the forage plots were of the same magnitude with values reported for grass cultivation in northern Europe (Maljanen et al., 2010). They were, however, 6–10 times higher than NEE reported for year 2002 in a 375 nearby field (Lohila et al., 2004), highlighting the spatial and temporal variation in soil emissions.

During the first two years of the experiment, the CH$_4$ fluxes of the forage plots were negative indicating net consumption of CH$_4$ by the soil microorganism. The CH$_4$ oxidation rates were generally higher than average values reported from Nordic cultivated peat soils which have shown net positive values for grass fields (Maljanen et al., 2007, 2010). There was a change from negative fluxes of CH$_4$ to relatively high emissions after the annual mean water table raised above -40 cm during the two 380 latter years of the experiment. However, compared to rewetted agricultural sites in the temperate zone, the values of ca. 8 kg CH$_4$-C per hectare were clearly lower than the average of 180 kg CH$_4$-C ha^{-1} yr^{-1} found in temperate paludiculture-like grassland ecosystems (Bianchi et al., 2021).

The N$_2$O emissions ranging from 6 to 12 kg N per hectare annually were typical for northern European grass fields on organic soils as they were within the 95% confidence interval of the reported values from temperate and boreal regions (Hiraishi et al., 385 2014). After the high emission peak in the beginning of the experiment there were only short-term peaks after fertilisation. One of them was especially high and long-lasting and likely induced by heavy rainfall after a long dry period coinciding with fertilisation in May-June 2022. It is typical that high peaks after fertilisation occur when fertilisation is followed by rainfall (Dobbie et al., 1999), and fertiliser-induced peaks may be totally absent if there is no coinciding rainfall (Beetz et al., 2013).

3.2 Set-aside

390 The set-aside plots with slowly evolving vegetation had clearly lower GP than the forage plots during the three first years. However, also the ER was lower in the set-aside, and the resulting NEE was of the same magnitude in both treatments. Because there was no biomass export from the set-aside the NECB was lower than in the forage treatment in most years. The modelled NEE values were about double compared to long-term abandoned croplands in the Nordic countries (Maljanen et al., 2010)

395 but in our study the plots did not represent similar ecosystems as they were "abandoned" only for a short period.

N_2O fluxes of the set-aside plots were extremely high in 2019 compared to results of previous studies on cultivated peat soils in Nordic countries (Maljanen et al., 2010). As the "set-aside" was fertilised and unsuccessfully planted with bog bilberry, the high emissions were likely due to abundant free mineral nitrogen in the absence of plant nutrient uptake. As the berry plants did not thrive, the soil was bare for a long period and the N_2O emissions remained higher than in the other treatments throughout

400 the summer. Such conditions were prevailing also in a similar bare fallow treatment at a nearby site in 2000-2002, yielding average N_2O emissions of 25 kg N ha^{-1} yr^{-1} (Regina et al., 2004). During the second year, the emissions lowered but as the plots were fertilised also in 2020, they still exhibited as high emissions as the forage plots. During the last two years the N_2O emissions were at a notably low level which likely resulted from ceasing of fertilisation and a slightly higher WTD leading to less peat being exposed to aerobic conditions. Raising the WTD has been found to diminish N_2O emissions in several studies

405 (Leppelt et al., 2014; van Beek et al., 2010).

3.3 Willow

Willow grew well at this site and the mean annual yields were in the higher end of the range 4-16 Mg ha^{-1} estimated for northern climate conditions (Viherä-Aarnio et al., 2022). Carbon lost in soil respiration was lower than the amount sequestered

410 in the willow biomass in all years except in 2019, leading to highly negative NEE during the whole rotation. However, the amount of carbon exported in harvest exceeded the NEE and the yielding NECB indicated net loss of carbon to the atmosphere. Although the average annual NECB calculated from the four-year carbon balance (1.9 Mg C ha^{-1} yr^{-1}) was low compared to the forage or set-aside treatments, it still indicated a climate-warming end result in short-rotation cropping of willow on peat soil. It is possible to achieve a net positive NEBC in willow cultivation on mineral soils (Harris et al., 2017; Morrison et al.,

415 2019) but in peatlands the high rate of soil respiration inevitably reduces this potential (Kasimir et al., 2018).

3.4 Considerations of the management options

The annual emissions can be compared to a well-drained cereal site (mean WTD 68 cm) on the same field plot (Honkanen et al., 2023), as the distance between these two experiments was just about 20 m. In 2020, when similar measurements were

420 conducted in both experiments, the total GHG balance (GWP100 with harvest) was 29 Mg in the set-aside and 43 Mg in the forage treatment while it was 39 Mg CO_2-eq. in the conventionally managed cereal plots. As the comparable figure for willow was 10 Mg in the willow treatment, it can be argued that the set-aside and willow cultivation with a moderate raise of WTD were better management options than cultivation of annual crops with a typical drainage depth. It was also clear that willow had the best GHG balance of these three management options, which is in agreement with findings of grassland and willow

425 cropping in southern England (Harris et al., 2017). However, the total emissions were still relatively high suggesting that this kind of moderately wet management is not an efficient climate mitigation measure. This was also shown by the modelling results of Kasimir et al. (2018) concluding that fully rewetted peatland had the most favourable carbon balance and less emissions from soil in a comparison of four different peatland management scenarios. However, management decisions, like cutting height also play a role in determining the final carbon balance in short-rotation cropping (Berhongaray et al., 2017).

430   Set-aside is a relevant management option to study because many cultivated peat fields end up as uncultivated plots when their drainage system degrades, and the landowner finds them too wet for cultivation. The annual total emissions were lower in the set-aside plots compared to the forage in 2020 and 2021, and also in 2022 if the carbon exported in harvest is taken into account. However, they were not especially low as compared to cultivated peat soils in general. Thus, leaving cultivated peat soils uncultivated without active rewetting is not desirable form of land management as these sites drift out from food

435   production, but the GHG emissions can remain high.

Our set-aside plots were actually intended to be vegetated by bog bilberry, a native mire plant that could become a novel antioxidant-rich ingredient for food (Lätti et al., 2010) or pharmaceutical (Esposito et al., 2019) industries. However, we soon noticed that the seedlings did not grow roots indicating that formerly agriculturally cultivated peat was not a suitable substrate for this plant. As the nutrient content of the topsoil did not show large deviations from the reported ranges supporting the

440   growth of bog bilberry (Jacquemart, 1996), it is likely that the pH of 5.4 at our site was too high. Bog bilberry is usually found in soils with pH below 5. However, in recent trials it has been successfully grown on Chinese farmlands with pH 5-6 but low pH improved the growth also there (Duan et al., 2022).

3.5 Uncertainties

445   There are usually high uncertainties in the GHG measurements, and this is especially true regarding the combination of methods chosen for the willow treatment. The carbon balance of willow was determined using a combination of the pool-based and flux-based methods, which can differ by several magnitudes (Berhongaray et al., 2017). The most reliable method for measuring the carbon balance of willow stands is likely the eddy covariance method, which is not feasible in plot experiments. Part of the uncertainty also arises from the simplicity of the models. For example, soil respiration was modelled only based on

450   soil temperature and WTD, although it can be affected also e.g. by changes in microbial community composition or activity (Yang et al. 2022) and soil moisture which does not always well follow changes in WTD (Smith et al. 2018). Estimating vegetation cover using measured LAI is also problematic, as it reflects weakly the amount of active chlorophyll (Delegido et al., 2015; Gregersen et al., 2013). It is especially difficult to assess active vegetation at the beginning and end of the growing season. However, the influence on the annual balance is minor due to low temperature and radiation at that time. With the

455   Canopeo application, the models were significantly better as it was possible to determine the green leaf area better than with the previously used LAI measurement with the SunScan instrument. The measurement results of PAR values feature uncertainties due to abrupt changes in cloudiness or fogging and dirt on the plexiglass. Due to technical problems, FMI data and another radiation meter was used to fill the gaps in the PAR measurements especially in 2021. The plexiglass surfaces were kept as clean as possible, fogging was kept low by using a short measurement time, and clear sky conditions were

460   preferred which should reduce the uncertainty occurred in measurements. Model predicted soil temperature in gap filling may cause some error, but the filled gaps were not long, and the error was mostly diurnal with low significance for the annual balances. Regarding biweekly N_2O and CH_4 measurements, there is a high risk of missing short-term peaks, for example due to freeze-thaw cycles (Lammirato et al., 2021). Also, if the measurements hit peaks, the emissions may be overestimated due to interpolation of the gaps in the data particularly during times with infrequent measurements.

465

4 Conclusions

The results indicate that wet management of cultivated peat soils considerable reduces the soil respiration and N_2O emissions. Significant counteracting effect of increased CH_4 emissions are also avoided as long as the WTD does not raise close to the soil surface. However, compared to full rewetting, partial rewetting remains a compromise solution to climate warming as it

470   is likely that the peat layer will eventually be lost. It is important to develop incentives to inundate large, connected peatland areas to ensure water availability and maintenance of high enough water table for efficient control of peat decomposition.

Authorship contributions. KL and HK designed the experiment. JH, HH, SS and TL developed the methodology. HK and TL planned, supervised and partly conducted the field work. KL, HH and HK analysed and visualised the data. KL and HH wrote the original manuscript. All authors were involved in revising the text.

Competing interests. The contact author has declared that none of the authors has any competing interests.

Acknowledgements. The authors are grateful to the technical staff of Natural Resources Institute Finland for skilled work in the field and laboratory.

Financial support. This study was part of the project SOMPA (Novel soil management practices – key for sustainable bioeconomy and climate change mitigation), funded by the Strategic Research Council at the Research Council of Finland, grant No 312912 and INSURE (Indicators for successful carbon sequestration and greenhouse gas mitigation by rewetting cultivated peat soils) subproject of the EJP Soil project that has received funding from the European Union's Horizon 2020 research and innovation programme under grant agreement No 862695.

490

References

Aparicio, N., Villegas, D., Casadesus, J., Araus, J. L., and Royo, C.: Spectral Vegetation Indices as Nondestructive Tools for Determining Durum Wheat Yield, Agron. J., 92, 83–91, https://doi.org/10.2134/agronj2000.92183x, 2000.

van Beek, C. L., Pleijter, M., Jacobs, C. M. J., Velthof, G. L., van Groenigen, J. W., and Kuikman, P. J.: Emissions of N2O from fertilized and grazed grassland on organic soil in relation to groundwater level, Nutr. Cycl. Agroecosystems, 86, 331–340, https://doi.org/10.1007/s10705-009-9295-2, 2010.

Beetz, S., Liebersbach, H., Glatzel, S., Jurasinski, G., Buczko, U., and Hoeper, H.: Effects of land use intensity on the full greenhouse gas balance in an Atlantic peat bog, Biogeosciences, 10, 1067–1082, https://doi.org/10.5194/bg-10-1067-2013, 2013.

Berhongaray, G., Verlinden, M. S., Broeckx, L. S., Janssens, I. A., and Ceulemans, R.: Soil carbon and belowground carbon balance of a short-rotation coppice: assessments from three different approaches, GCB Bioenergy, 9, 299–313, https://doi.org/10.1111/gcbb.12369, 2017.

Bianchi, A., Larmola, T., Kekkonen, H., Saarnio, S., and Lang, K.: Review of Greenhouse Gas Emissions from Rewetted Agricultural Soils, WETLANDS, 41, 108, https://doi.org/10.1007/s13157-021-01507-5, 2021.

Bockermann, C., Eickenscheidt, T., and Droesler, M.: Adaptation of fen peatlands to climate change: rewetting and management shift can reduce greenhouse gas emissions and offset climate warming effects, BIOGEOCHEMISTRY, https://doi.org/10.1007/s10533-023-01113-z, 2024.

Boonman, C. C. F., Heuts, T. S., Vroom, R. J. E., Geurts, J. J. M., and Fritz, C.: Wetland plant development overrides nitrogen effects on initial methane emissions after peat rewetting, Aquat. Bot., 184, 103598, https://doi.org/10.1016/j.aquabot.2022.103598, 2023.

Delegido, J., Verrelst, J., Rivera, J. P., Ruiz-Verdú, A., and Moreno, J.: Brown and *green* LAI mapping through spectral indices, Int. J. Appl. Earth Obs. Geoinformation, 35, 350–358, https://doi.org/10.1016/j.jag.2014.10.001, 2015.

Dobbie, K. E., McTaggart, I. P., and Smith, K. A.: Nitrous oxide emissions from intensive agricultural systems: Variations between crops and seasons, key driving variables, and mean emission factors, J. Geophys. Res. Atmospheres, 104, 26891–26899, https://doi.org/10.1029/1999JD900378, 1999.

Duan, Y., Guo, B., Zhang, L., Li, J., Li, S., Zhao, W., Yang, G., Zhou, S., Zhou, C., Song, P., Li, P., Fang, L., Hou, S., Shi, D., Zhao, H., and Guo, P.: Interactive climate-soil forces shape the spatial distribution of foliar N:P stoichiometry in Vaccinium uliginosum planted in agroforests of Northeast China, Front. Ecol. Evol., 10, https://doi.org/10.3389/fevo.2022.1065680, 2022.

520   Esposito, D., Overall, J., and Grace, M. H.: Alaskan Berry Extracts Promote Dermal Wound Repair Through Modulation of Bioenergetics and Integrin Signaling, Front. Pharmacol., 10, https://doi.org/10.3389/fphar.2019.01058, 2019.

Evans, C. D., Peacock, M., Baird, A. J., Artz, R. R. E., Burden, A., Callaghan, N., Chapman, P. J., Cooper, H. M., Coyle, M., Craig, E., Cumming, A., Dixon, S., Gauci, V., Grayson, R. P., Helfter, C., Heppell, C. M., Holden, J., Jones, D. L., Kaduk, J., Levy, P., Matthews, R., McNamara, N. P., Misselbrook, T., Oakley, S., Page, S. E., Rayment, M., Ridley, L. M., Stanley,
525   K. M., Williamson, J. L., Worrall, F., and Morrison, R.: Overriding water table control on managed peatland greenhouse gas emissions, Nature, https://doi.org/10.1038/s41586-021-03523-1, 2021.

Freeman, B. W. J., Evans, C. D., Musarika, S., Morrison, R., Newman, T. R., Page, S. E., Wiggs, G. F. S., Bell, N. G. A., Styles, D., Wen, Y., Chadwick, D. R., and Jones, D. L.: Responsible agriculture must adapt to the wetland character of mid-latitude peatlands, Glob. Change Biol., 28, 3795–3811, https://doi.org/10.1111/gcb.16152, 2022.

530   Gregersen, P. L., Culetic, A., Boschian, L., and Krupinska, K.: Plant senescence and crop productivity, Plant Mol. Biol., 82, 603–622, https://doi.org/10.1007/s11103-013-0013-8, 2013.

Guenther, A., Barthelmes, A., Huth, V., Joosten, H., Jurasinski, G., Koebsch, F., and Couwenberg, J.: Prompt rewetting of drained peatlands reduces climate warming despite methane emissions, Nat. Commun., 11, 1644–1644, https://doi.org/10.1038/s41467-020-15499-z, 2020.

535   Harris, Z. M., Alberti, G., Viger, M., Jenkins, J. R., Rowe, R., McNamara, N. P., and Taylor, G.: Land-use change to bioenergy: grassland to short rotation coppice willow has an improved carbon balance, GCB Bioenergy, 9, 469–484, https://doi.org/10.1111/gcbb.12347, 2017.

Hiraishi, T., Krug, T., Tanabe, K., Srivastava, N., Baasansuren, J., Fukuda, M., and Troxler, T. G.: Supplement to the 2006 IPCC guidelines for national greenhouse gas inventories: Wetlands, IPCC, Switzerland, 2014.

540   Honkanen, H., Kekkonen, H., Heikkinen, J., Kaseva, J., and Lång, K.: Minor effects of no-till treatment on GHG emissions of boreal cultivated peat soil, Biogeochemistry, https://doi.org/10.1007/s10533-023-01097-w, 2023.

Huang, Y., Ciais, P., Luo, Y., Zhu, D., Wang, Y., Qiu, C., Goll, D. S., Guenet, B., Makowski, D., De Graaf, I., Leifeld, J., Kwon, M. J., Hu, J., and Qu, L.: Tradeoff of CO2 and CH4 emissions from global peatlands under water-table drawdown, Nat. Clim. Change, 11, 618–622, https://doi.org/10.1038/s41558-021-01059-w, 2021.

545   Humpenöder, F., Karstens, K., Lotze-Campen, H., Leifeld, J., Menichetti, L., Barthelmes, A., and Popp, A.: Peatland protection and restoration are key for climate change mitigation, Environ. Res. Lett., 15, 104093, https://doi.org/10.1088/1748-9326/abae2a, 2020.

Jacquemart, A.-L.: Vaccinium Uliginosum L., J. Ecol., 84, 771–785, https://doi.org/10.2307/2261339, 1996.

Jokinen, P., Pirinen, P., Kaukoranta, J.-P., Kangas, A., Alenius, P., Eriksson, P., Johansson, M., and Wilkman, S.: Tilastoja
550   Suomen ilmastosta ja merestä 1991-2020, Ilmatieteen laitos, 2021.

Kandel, T. P., Elsgaard, L., and Laerke, P. E.: Measurement and modelling of CO2 flux from a drained fen peatland cultivated with reed canary grass and spring barley, Glob. Change Biol. Bioenergy, 5, 548–561, https://doi.org/10.1111/gcbb.12020, 2013.

Kandel, T. P., Karki, S., Elsgaard, L., Labouriau, R., and Laerke, P. E.: Methane fluxes from a rewetted agricultural fen
555   during two initial years of paludiculture, Sci. Total Environ., 713, 136670–136670, https://doi.org/10.1016/j.scitotenv.2020.136670, 2020.

Karki, S., Elsgaard, L., Audet, J., and Laerke, P. E.: Mitigation of greenhouse gas emissions from reed canary grass in paludiculture: effect of groundwater level, Plant Soil, 383, 217–230, https://doi.org/10.1007/s11104-014-2164-z, 2014.

Kasimir, Å., He, H., Coria, J., and Nordén, A.: Land use of drained peatlands: Greenhouse gas fluxes, plant production, and
560   economics, Glob. Change Biol., 24, 3302–3316, https://doi.org/10.1111/gcb.13931, 2018.

Kutzbach, L., Schneider, J., Sachs, T., Giebels, M., Nykanen, H., Shurpali, N. J., Martikainen, P. J., Alm, J., and Wilmking, M.: CO2 flux determination by closed-chamber methods can be seriously biased by inappropriate application of linear regression, Biogeosciences, 4, 1005–1025, https://doi.org/10.5194/bg-4-1005-2007, 2007.

565 Lammirato, C., Wallman, M., Weslien, P., Klemedtsson, L., and Rütting, T.: Measuring frequency and accuracy of annual nitrous oxide emission estimates, Agric. For. Meteorol., 310, 108624, https://doi.org/10.1016/j.agrformet.2021.108624, 2021.

Lätti, A. K., Jaakola, L., Riihinen, K. R., and Kainulainen, P. S.: Anthocyanin and Flavonol Variation in Bog Bilberries (Vaccinium uliginosum L.) in Finland, J. Agric. Food Chem., 58, 427–433, https://doi.org/10.1021/jf903033m, 2010.

Lehtonen, H., Huan-Niemi, E., and Niemi, J.: The transition of agriculture to low carbon pathways with regional distributive
570 impacts, Environ. Innov. Soc. Transit., 44, 1–13, https://doi.org/10.1016/j.eist.2022.05.002, 2022.

Leifeld, J. and Menichetti, L.: The underappreciated potential of peatlands in global climate change mitigation strategies, Nat. Commun., 9, 1071–1071, https://doi.org/10.1038/s41467-018-03406-6, 2018.

Leppelt, T., Dechow, R., Gebbert, S., Freibauer, A., Lohila, A., Augustin, J., Droesler, M., Fiedler, S., Glatzel, S., Hoeper, H., Jaerveoja, J., Laerke, P. E., Maljanen, M., Mander, U., Maekiranta, P., Minkkinen, K., Ojanen, P., Regina, K., and
575 Stromgren, M.: Nitrous oxide emission budgets and land-use-driven hotspots for organic soils in Europe, Biogeosciences, 11, 6595–6612, https://doi.org/10.5194/bg-11-6595-2014, 2014.

Liu, W., Fritz, C., Van Belle, J., and Nonhebel, S.: Production in peatlands: Comparing ecosystem services of different land use options following conventional farming, Sci. Total Environ., 875, 162534, https://doi.org/10.1016/j.scitotenv.2023.162534, 2023.

580 LLOYD, J. and TAYLOR, J.: On the Temperature-Dependence of Soil Respiration, Funct. Ecol., 8, 315–323, https://doi.org/10.2307/2389824, 1994.

Lohila, A., Aurela, M., Regina, K., and Laurila, T.: Soil and total ecosystem respiration in agricultural fields: effect of soil and crop type, Plant Soil, 251, 303–317, https://doi.org/10.1023/A:1023004205844, 2003.

Lohila, A., Aurela, M., Tuovinen, J., and Laurila, T.: Annual CO2 exchange of a peat field growing spring barley or
585 perennial forage grass, J. Geophys. Res.-Atmospheres, 109, D18116–D18116, https://doi.org/10.1029/2004JD004715, 2004.

Long, S. P. and Hällgren, J.-E.: Measurement of CO2 assimilation by plants in the field and the laboratory, in: Photosynthesis and Production in a Changing Environment: A field and laboratory manual, edited by: Hall, D. O., Scurlock, J. M. O., Bolhàr-Nordenkampf, H. R., Leegood, R. C., and Long, S. P., Springer Netherlands, Dordrecht, 129–167, https://doi.org/10.1007/978-94-011-1566-7_9, 1993.

590 Maljanen, M., Liikanen, A., Silvola, J., and Martikainen, P.: Measuring N2O emissions from organic soils by closed chamber or soil/snow N2O gradient methods, Eur. J. Soil Sci., 54, 625–631, https://doi.org/10.1046/j.1365-2389.2003.00531.x, 2003.

Maljanen, M., Hytonen, J., Makiranta, P., Alm, J., Minkkinen, K., Laine, J., and Martikainen, P. J.: Greenhouse gas emissions from cultivated and abandoned organic croplands in Finland, Boreal Environ. Res., 12, 133–140, 2007.

595 Maljanen, M., Sigurdsson, B. D., Guomundsson, J., Oskarsson, H., Huttunen, J. T., and Martikainen, P. J.: Greenhouse gas balances of managed peatlands in the Nordic countries - present knowledge and gaps, Biogeosciences, 7, 2711–2738, https://doi.org/10.5194/bg-7-2711-2010, 2010.

Mander, U., Espenberg, M., Melling, L., and Kull, A.: Peatland restoration pathways to mitigate greenhouse gas emissions and retain peat carbon, BIOGEOCHEMISTRY, https://doi.org/10.1007/s10533-023-01103-1, 2023.

600 Meek, D. W., Hatfield, J. L., Howell, T. A., Idso, S. B., and Reginato, R. J.: A Generalized Relationship between Photosynthetically Active Radiation and Solar Radiation1, Agron. J., 76, 939–945, https://doi.org/10.2134/agronj1984.00021962007600060018x, 1984.

Morrison, R., Rowe, R. L., Cooper, H. M., and McNamara, N. P.: Multi-year carbon budget of a mature commercial short rotation coppice willow plantation, GCB Bioenergy, 11, 895–909, https://doi.org/10.1111/gcbb.12608, 2019.

605 Pacaldo, R. S., Volk, T. A., and Briggs, R. D.: Carbon Sequestration in Fine Roots and Foliage Biomass Offsets Soil CO2 Effluxes along a 19-year Chronosequence of Shrub Willow (Salix x dasyclados) Biomass Crops, BioEnergy Res., 7, 769–776, https://doi.org/10.1007/s12155-014-9416-x, 2014.

Raich, J. W., Rastetter, E. B., Melillo, J. M., Kicklighter, D. W., Steudler, P. A., Peterson, B. J., Grace, A. L., Moore III, B., and Vorosmarty, C. J.: Potential Net Primary Productivity in South America: Application of a Global Model, Ecol. Appl., 1, 610 399–429, https://doi.org/10.2307/1941899, 1991.

Regina, K., Syvasalo, E., Hannukkala, A., and Esala, M.: Fluxes of N2O from farmed peat soils in Finland, Eur. J. Soil Sci., 55, 591–599, https://doi.org/10.1111/j.1365-2389.2004.00622.x, 2004.

Strack, M., Davidson, S. J., Hirano, T., and Dunn, C.: The Potential of Peatlands as Nature-Based Climate Solutions, Curr. Clim. Change Rep., 8, 71–82, https://doi.org/10.1007/s40641-022-00183-9, 2022.

615 Tanneberger, F., Birr, F., Couwenberg, J., Kaiser, M., Luthardt, V., Nerger, M., Pfister, S., Oppermann, R., Zeitz, J., Beyer, C., van der Linden, S., Wichtmann, W., and Närmann, F.: Saving soil carbon, greenhouse gas emissions, biodiversity and the economy: paludiculture as sustainable land use option in German fen peatlands, Reg. Environ. Change, 22, 69, https://doi.org/10.1007/s10113-022-01900-8, 2022.

Viherä-Aarnio, A., Jyske, T., and Beuker, E.: Pajut biokiertotaloudessa - Materiaaleja, arvoaineita, ympäristöhyötyjä : 620 Synteesiraportti, Luonnonvarakeskus, 2022.

Vuorinen, J. and Mäkitie, O.: The method of soil testing in use in Finland, Maatalouskoelaitoksen maatutkimusosasto, Helsinki, 44 pp., 1955.

Wilson, D., Blain, D., Couwenberg, J., Evans, C., Murdiyarso, D., Page, S., Renou-Wilson, F., Rieley, J., Strack, M., and Tuittila, E.: Greenhouse gas emission factors associated with rewetting of organic soils, Mires Peat, 14, 1–28, 2016.

625 Zheng, D., Hunt, E., and Running, S.: A daily soil temperature model based on air temperature and precipitation for continental applications, Clim. Res., 2, 183–191, https://doi.org/10.3354/cr002183, 1993.